Ternary cobalt-molybdenum-zirconium coatings: electrolytic deposition and functional properties

N. Sakhnenko[*], M. Ved, M. Koziar

*National Technical University "Kharkov Polytechnic Institute",
2, Kyrpychova Str., 61002, Kharkiv, Ukraine*
e-mail: sakhnenko@kpi.kharkov.ua

Consistent patterns for electrodeposition of Co-Mo-Zr coatings from polyligand citrate-pyrophosphate bath were investigated. The effect of both current density amplitude and pulse on/off time on the quality, composition and surface morphology of the galvanic alloys were determined. It was established the coating Co-Mo-Zr enrichment by molybdenum with current density increasing up to 8 A·dm^{-2} as well as the rising of pulse time and pause duration promotes the content of molybdenum because of subsequent chemical reduction of its intermediate oxides by hydrogen ad-atoms. It was found that the content of the alloying metals in the coating Co-Mo-Zr depends on the current density and on/off times extremely and maximum Mo and Zr content corresponds to the current density interval 4–6 A·dm^{-2}, on-/off-time 2–10 ms. It was shown that Co-Mo-Zr alloys exhibits the greatest level of catalytic properties as cathode material for hydrogen electrolytic production from acidic media which is not inferior a platinum electrode. The galvanic alloys Co-Mo-Zr with zirconium content 2–3 at.% demonstrate high catalytic properties in the carbon(II) oxide conversion. This confirms the efficiency of materials as catalysts for the gaseous wastes purification and gives the reason to recommend them as catalysts for hydrocarbon combustion.

Key words: cobalt ternary coatings, molybdenum, zirconium, citrate-pyrophosphate bath, catalytic properties, corrosion resistance, electrodeposition, hydrogen evolution reaction, pulse electrolysis
PACS: 61.46.+w

Introduction

Energetic security of any country is based on the several factors, among which there are the network of national energy generating enterprises, developed industrial basis on the energy accumulating devices and energy sources production. Eco-friendly fuel cells (FC) are among the promising renewable energy sources, however, the high cost of the noble metal electrodes prevents their dissemination and widespread use [1, 2]. Development of the fuel cells and flow battery at various red-ox systems (RFB) needs to create effective catalytically active electrodes on the basis of transition metals [3, 4]. Among the most important requirements to electrode materials of FC and RFB are: chemical stability of the surface and inactivity to technological environment components; wide window of polarization potentials, in which electrode stays inactive; high selectivity and catalytic activity toward main electrode reactions; significant specific surface area. Even brief review gives an impression that electrode materials that are being used in these electrochemical systems are not optimized [5, 6]. For instance, one of the most

widespread electrode material for FC and FRB is a number of carbon modifications – graphite, carbon fibers, porous and pressed carbon, carbon cloth, graphite with thermally or chemically modified surface, nickel foam, platinum or platinum titanium, oxides of platinum group metals, etc [7–10]. It is worth mentioning that in scientific literature for the last years there are too few publications on electrode materials on the basis of hi-tech materials, such as nanostructured and nanocrystalline materials based on the corrosion resistant amorphous metal alloys (metal glass), or nanostructured deposits by synergistic alloys [11–13]. The most efficient directions of catalytic materials synthesis by physic-inorganic chemistry methods are electrochemical technologies that provide the opportunity to very flexibly control the component content, the rate of deposition, the state of the surface, by varying the electrolyte composition and polarization mode (static or pulse, reverse current or decrease of the potential) [14–16]. Utilization of the electrochemical methods favors the interactions in the chain "process parameters – composition and structure of the material – properties – functions – application". Because of this it is possible to

fabricate the deposits of varied qualitative and quantitative composition and with desirable functional properties (synergistic or additive), such as microhardness, wear-, thermo-, chemical and corrosion resistance, catalytic activity, etc [17–20]. When synthesizing new and improving existing catalysts it is necessary to determine the factors influencing the catalytic activity and especially the nature of the catalyst, since electro-catalytic activity depends on chemical composition and state of the surface (amorphous, crystalline, grain size, etc.) [21–23].

It has previously been shown prospects of electrolytic binary cobalt alloys with molybdenum or tungsten to produce hydrogen by alkali electrolysis [24, 25] as well as to the oxidation of hydrocarbons [26, 27]. However, it is of interest to create catalytic materials based on ternary synergistic cobalt alloys with metals of differing affinity to oxygen and hydrogen and high corrosion resistance for use as catalysts, and electrode materials for fuel and flow batteries.

The aim of this work is to study the influence of the electrolysis parameters on the quality, composition, morphology, catalytic properties and corrosion resistance of ternary galvanic Co-Mo-Zr coatings.

Experimental

Coatings were deposited onto the substrates out of steel. Pretreatment of samples included grinding, degreasing in a solution of sodium carbonate at 50 ºC, and washing, etching in a mixture of hydrochloric acid and sulfuric acid at a temperature of 20 º C and thoroughly washing in flowing water.

Deposits of cobalt with molybdenum and tungsten or zirconium were formed at temperatures of 25–50°C from a complex polyligand citrate-diphosphate bath. The coatings Co-Mo-Zr were deposited from electrolyte composition (M): cobalt sulfate 0.15, sodium molybdate 0.06, zirconium (IV) sulfate 0.05, sodium citrate 0.2, and potassium diphosphate 0.1. The pH value of electrolytes was adjusted within the range 8–9 by sodium hydroxide. Electrolytes were prepared from analytically pure reagents: $CoSO_4 \cdot 7H_2O$, $Na_2MoO_4 \cdot 2H_2O$, $Zr(SO_4)_2 \cdot 4H_2O$, $K_4P_2O_7$, $Na_3C_6H_5O_7 \cdot 2H_2O$ dissolved in a small amount of distilled water following by solution mixture in a certain sequence, based on the ionic equilibrium study results [28].

The deposits were formed in pulsed mode with unipolar pulse current of amplitude 2–15 $A \cdot dm^{-2}$ in the frequency f range of 19−910 Hz at a pulse duration $t_{on} = 2−50$ ms and pause time $t_{off} = 5−50$ ms, duty factor $q = (t_{on} + t_{of})/t_{on}$ was 2−26. Coplanar cobalt plates were used as anodes. The cathode-to-anode area ratio was kept at 1:5. The pulse electrolysis was performed using pulse current supply unit (ZY-100 ± 12). The electrode potentials were measured relative to an EVL-1M1 silver chloride reference electrode connected to the working cell via a salt bridge filled with saturated potassium chloride solution jellied with Ceylon gelatin. The potentials presented in the paper are given relative to the standard hydrogen electrode (SHE).

The electrodeposition current efficiency Ce (%) was determined from the weight and chemical composition of the deposited alloys and the charge passed using the electrochemical equivalent of the alloy. The thickness of the deposits was calculated from a sample actual weight increase after the electrolysis.

The chemical composition of the coatings was determined by energy dispersive X-ray spectroscopy on an Oxford INCA Energy 350 electron probe microanalysis integrated into the system of the SEM. The X-rays were excited by exposure of the samples to a beam of 15 keV electrons. The surface morphology of the deposits was studied with a Zeiss EVO 40XVP scanning electron microscope (SEM). Images were recorded by the registration of secondary electrons (SEs) via scanning with an electron beam; this mode made it possible to study the topography with a high resolution and contrast ratio. The surface roughness was evaluated by the contact method on $10 \times 10 \times 2$ mm samples with an NT-206 scanning probe AFM microscope (lateral and vertical resolutions 2 and 0.2 nm, respectively; 1024×1024 scanning matrix, CSC cantilever B as probe, probe tip radius 10 nm).

The structure of the deposits was examined by X-ray diffraction analysis using a diffractometer (DRON-2.0) in the emission of iron anode and CuKα radiation.

Corrosion tests of the deposits were carried out in a model media with 1 M sodium sulfate with the addition of sulfuric acid to pH 3 or potassium hydroxide to pH 11 and in 3% potassium chloride (pH 7). The corrosion current was determined by the polarization resistance technique using digital analysis of anodic and cathodic plots in Tafel coordinates within the range 200−300 mV from

steady-state potential [29]. The potentiostat IPC-Pro controlled by PC was used for voltammetry measurements with scan rate 1 mV/sec^{-1}. Corrosion depth index k_h (mm per year) was converted from corrosion current:

$$k_h = (8.76 k_e i_{cor})/\rho,$$

where k_e − the electrochemical equivalent of alloy, kg/C^{-1}; i_{cor} − corrosion current density, A/m^{-2}; ρ − density of the alloy, kg/m^{-3}.

Electrochemical equivalent k_e and density ρ of the alloys were determined considering their quantitative composition [30].

Electro catalytic properties of covers were studied in model reaction of electrolytic hydrogen evolution from acidic and alkali media. The hydrogen current exchange density i_H^0 is utilized as the criteria of electrochemical catalysis since this parameter is independent of the electrode potential. Experimentally i_H^0 was determined at the point of intersection of the linear portion of the cathodic polarization dependence in Tafel coordinates at zero over potential [28]. The testing of catalytic properties was also carried out in the process of the carbon (II) oxide oxidation in a tubular flow reactor fabricated from quartz glass with the coaxially situated heating element. Initial mixture of CO (1 vol.%) and air was supplied to the reactor inlet at a rate of 0.025 dm^3·min^{-1}. Reactor temperature was increased gradually from 20 to 420 °C. Content of CO in the final mixture was analyzed using the indicator-analyzer "Dozor" [26].

Theoretic aspects

It was shown in previous papers [28, 31] the necessity of using polyligand electrolyte for the co-deposition of cobalt with molybdenum and zirconium because of the significant potential difference for alloying components. Citrate (Cit) and diphosphate ions that are indifferent to electrochemical oxidation and reduction in wide potential window and create coordination with many single and polyvalent ions are selected as ligands. The pH maintaining in the interval 8–9 is recommended for stable diphosphate (pK[CoP$_2$O$_7$]$^{2-}$=6.1) and citrate (pK[CoCit]$^-$=5.0) complexes since the strength of compounds depends on the ligands protonation. Moreover, in a weakly alkaline medium Mo (VI) is a mono-oxometalate

ion MoO_4^{2} [16, 31] and zirconium predominantly is ZrO^{2+}. These particles are involved in the formation of the heteronuclear complexes with cobalt discharging at the cathode by induced co-deposition [32].

It was shown in previous studies [28] we can obtain ternary Co galvanic deposits and control their composition by changing the concentration ratio of salts of alloying metals and ligands in a bath, and electrolyte pH. We need to keep in mind that formation of heteronuclear complexes of cobalt with molybdenum and zirconium with citrate and diphosphate ligands and their subsequent reduction in the alloy may be competing as it was shown for iron ternary deposits [20].

Taking into account the considerable difference of alloying components' redox potentials (Table 1) and their step reduction conjugated with chemical reaction as it was shown in [16, 23, 31] preference is given to forming ternary coatings using pulse electrolysis mode. Thus, energy and time parameters of the electrolysis can be an effective instrument for control the composition and surface morphology, and hence the properties of ternary coatings especially catalytic activity and corrosion resistance.

Results and discussion

Increase the current density amplitude i of 2 to 4 A·dm^{-2} rises the Molybdenum content in the deposit Co-Mo-Zr up to ω(Mo)=24 at.% (Figure 1 a) reaching the concentration plateau at 24–25 at.% at current densities of 4–8 A·dm^{-2}. Coating enrichment by this alloying component with increasing current density is entirely predictable since the reduction of molybdate is at least a complex multi-step process accompanied by chemical reduction of intermediate Molybdenum oxides with Hydrogen ad-atoms H$_{ad}$ [23]. As we see from (Figure 1 b) the potential of the cathode at electrodeposition of the coatings Cobalt-Molybdenum-Zirconium is in the range − (2.0–2.8) V. Thus with increasing current density electrode potential shifts in the negative direction resulting in faster parallel reaction of Hydrogen reduction to form H$_{ad}$ which are involved in a chemical step of intermediate Molybdenum oxides reduction. Due to these processes the Molybdenum content in the deposits is increased. However, at current densities above 8 A·dm^{-2} reaction of Hydrogen evolution becomes the dominant as evidenced by the current efficiency (Figure 1 b)

whereby the molybdenum content in the alloy decreases.

The dependence of the Zirconium content in the ternary coatings from current amplitude i has an extreme character with a maximum $\omega(Zr)=3.6–3.7$ at% at current densities 4 A·dm^{-2} (Figure 1 a). It should be stated that when the amplitude of the current is higher than of 4 dm^{-2} there is a competitive deposition of Molybdenum and Zirconium in the coating, which is obviously due to the different mechanism of alloying metals reduction from polyligand electrolytes. Indeed, molybdenum reduction requires the transfer of 6 electrons accompanied by the removal of 4

coordinated oxygen atoms. Zirconium is likely included in the deposit in the form of oxygen compounds, which follows from the higher binding energy Zr–O [33-35] and confirmed by analysis of the composition of the surface layers.

A similar nonlinear relationship was observed for current efficiency of the ternary alloy Ce vs i (Fig 1 b): Ce increases by 20 % and reaches 63 % with rising current density from 5 to 8 A·dm^{-2}; however further increase in i reduces the current efficiency up to 47 %. Such behavior may be attributed with acceleration of site Hydrogen evolution reaction at higher current amplitude.
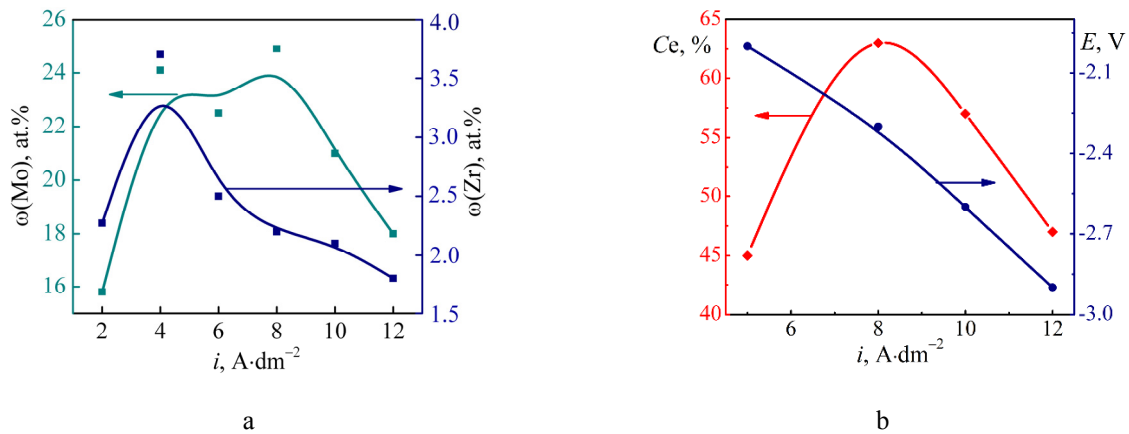
Figure 1 – Pulse current density influence on the composition (a) and current efficiency (b) for Co-Mo-Zr coatings; t_{on}/t_{off} 2/10 ms; T 20–25 °C; pH 8; plated time 30 min

Time parameters of pulsed electrolysis (duration of pulse t_{on} and pause t_{off}) strongly affect the composition and current efficiency of multicomponent deposits. Thus, the minimum value t_{on} should be sufficient to achieve the potential of metals co-deposition in the alloy, and the maximum – to ensure quality coatings and efficiency of electrolysis.

It was found that with increasing pulse time of 0.5 to 2 ms at a constant current density i=4 A·dm^{-2} and pause duration t_{off}=10 ms both Molybdenum and Zirconium content in the Co-Mo-Zr deposits grow (Figure 2 a). This is due to an increase in active current at the expense of a full signal handling, thereby achieving potential of alloying metals reduction in alloy. Increasing the pulse duration of more than 2 ms does not contribute to the growth of the above metals content in the

coating. Moreover, the zirconium content decreases with pulse duration exceeding 2 ms.

Prolong pause of 5 to 10 ms at a constant current density and pulse duration (t_{on} 2 ms) provides growth zirconium content in the alloy from 2.1 to 3.7 at.% which is followed by decreasing of $\omega(Zr)$ at larger current interruption (Figure 2 b). So the maximum concentration of Zirconium in the electrolytic alloy is reached under the ratio t_{on}/t_{off} = 2 / 10 ms (duty factor q = 10, f = 85 Hz). At the same time, the content of molybdenum in Co-Mo-Zr deposits regularly increases from 16.0 to 24.0 at% with the duration of the pause due to more complete chemical reduction of intermediate oxides by H_{ad} (Figure 2 b). It also shows the different mechanism of Zirconium and Molybdenum reduction and confirms their competitive co-deposition in the ternary coating under studied conditions.
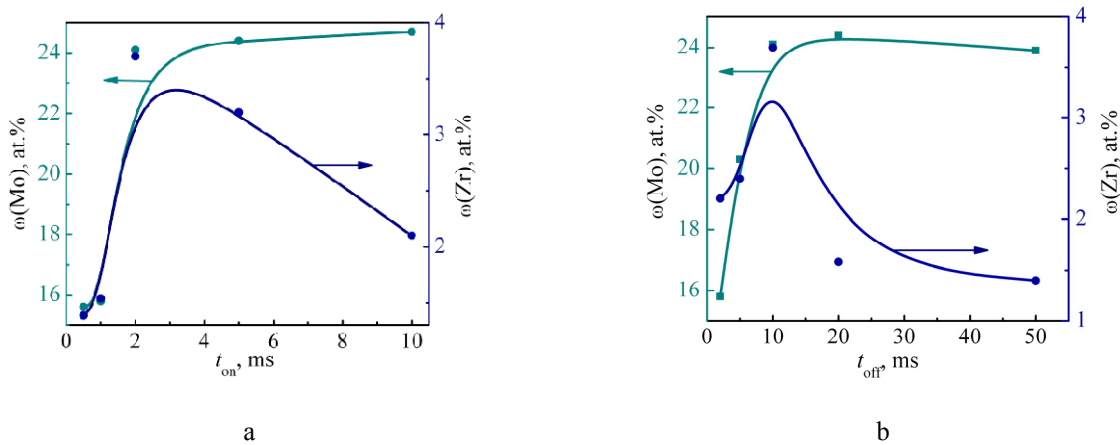
Figure 2 – Dependence of Co-Mo-Zr coating composition on the time of pulse t_{on} (a)
(t_{off} 10 ms) and pause t_{off} (b) (t_{on} 2 ms); i=4 A·dm^{-2}; T = 20–25 °C; pH 8; plated time 30 min

Current efficiency logically decreases of 60 to 36 % with increasing pulse time of 4 to 10 A·dm^{-2} due to the hydrogen evolution enhancement at a higher polarization. Prolong the pause positively influences the current efficiency of Cobalt-Molybdenum-Zirconium alloy as subsequent chemical reactions accompanying the alloying metals discharge are more fully but a larger current interruption reduces the efficiency of the process. Thus, current efficiency reaches 98 % when t_{off} = 50 ms and t_{on} = 2 ms.

Increasing the amplitude of the current changes the surface morphology and amplified internal stress that leads to fracture grid (Figure 3). The Figure 3 shows the surface becomes less smooth and more globular, and the crystallite sizes increase exactly due to the higher content of Molybdenum in the deposits. It should be emphasized sufficiently uniform distribution of the coating components on uneven relief, which may be attributed to a good dispersive capacity of the electrolyte. Increasing pulse time at a constant pause promotes the formation of spheroids on the surface but increasing tension in the coating and micro cracks become larger. Furthermore, some pores appear in coatings when the pulse time of 10 ms and the current density at 6–8 A·dm^{-2} (Figure 3 b, c), apparently due to hydrogen evolution.

The AFM analysis topography of the coatings Co-Mo-Zr show that their surface includes the parts of different morphology as one can see from Figure 4. The surface is characterized by globular structure with an average size of grains and crystallites 100–200 nm and singly located cone-shaped (Figure 4 a) or semi-spheroid (Figure 4 c) hills with a base diameter of 1–3 μm and a height of 0.5–1.5 μm. As appears from 2D- and 3D-topography maps of surface (Figure 4) the cone-shaped hills are formed of the smaller spheroids. Such globular surface is caused by the presence of molybdenum in the deposits as it was shown in [20, 24] and we can see rather uniform distribution of alloying elements at picks and valleys (Figure 4 b, c) on the surface with a slight predominance of Mo and Zr at picks. As the current density increases the number of spheroids at the deposits surface is also increased but both their height and diameter are reduced (Figure 4 c).

$t_{on}/t_{off} = 2/10$
Co − 72.2
Mo − 24.1
Zr − 3.7

$t_{on}/t_{off} = 5/10$
Co − 72.4
Mo − 24.4
Zr − 3.2

$t_{on}/t_{off} = 10/10$
Co − 73.2
Mo − 24.7
Zr − 2.1

$t_{on}/t_{off} = 10/20$
Co − 75.6
Mo − 21.9
Zr − 2.4

a

$t_{on}/t_{off} = 2/10$
Co − 75.0
Mo − 22.5
Zr − 2.5

$t_{on}/t_{off} = 5/10$
Co − 77.5
Mo − 20.1
Zr − 2.4

$t_{on}/t_{off} = 10/10$
Co − 71.1
Mo − 26.3
Zr − 2.6

b

$t_{on}/t_{off} = 2/10$
Co − 72.9
Mo − 24.9
Zr − 2.2

$t_{on}/t_{off} = 5/10$
Co − 76.7
Mo − 21.6
Zr − 1.7

$t_{on}/t_{off} = 10/10$
Co − 76.8
Mo − 20.6
Zr − 2.6

c
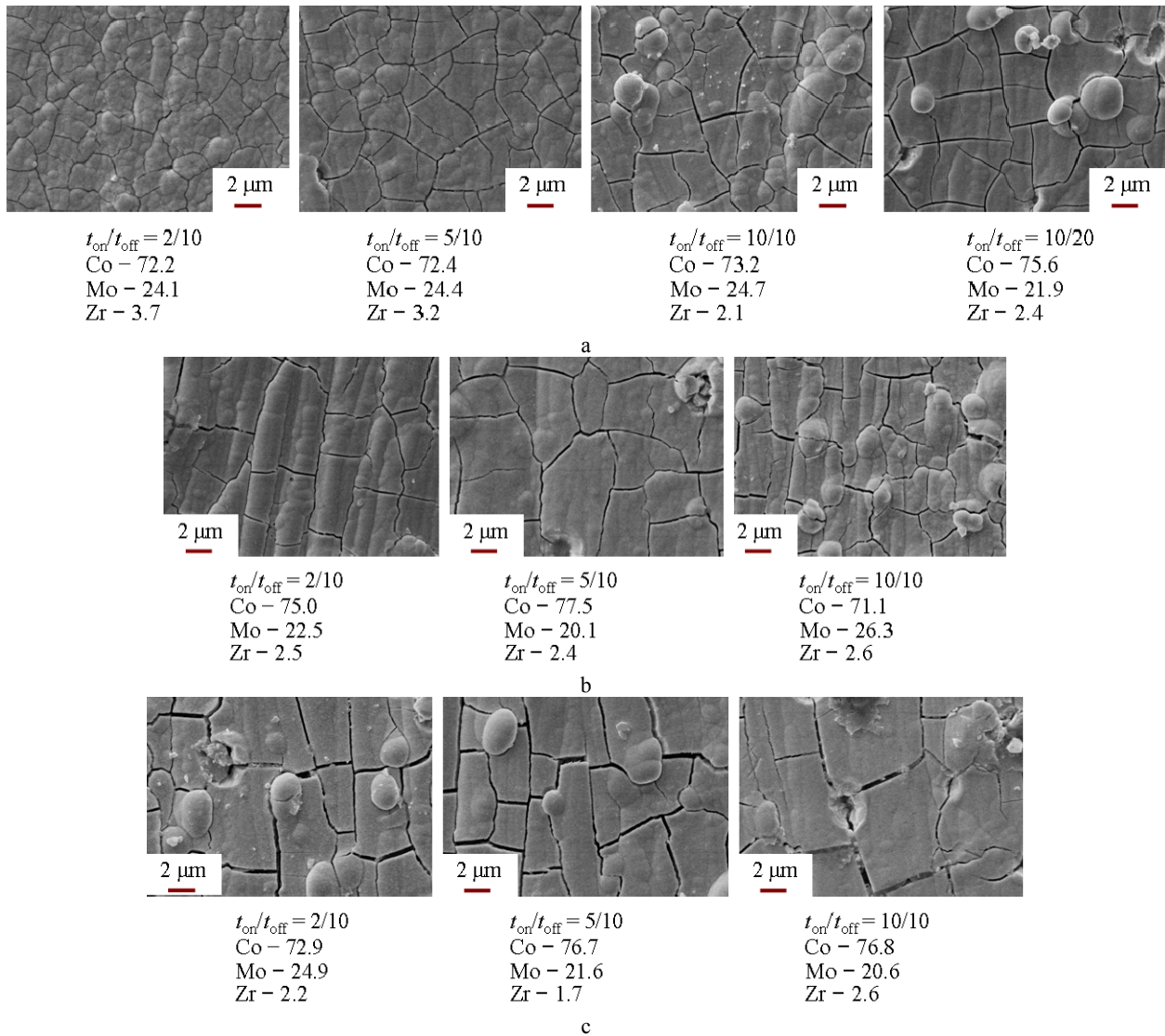
Figure 3 – Morphology (x2000) and composition (at.%) of Co-Mo-Zr coatings deposited in pulse mode at current density. $A \cdot dm^{-2}$: 4 (a); 6 (b) and 8 (c); T = 20–25 °C; pH 8; plated time 30 min

The parameters of surface roughness R_a=0.29 and R_q=0.38 for ternary coatings deposited at current density 4 $A \cdot dm^{-2}$ not differ from R_a=0.29 and R_q=0.4 for 6 $A \cdot dm^{-2}$. According to the R_a and R_q the Co-Mo-Zr electrolytic coatings have a surface roughness class of 8–9. Such developed surface of globular structure as well as composition of material may be associated with high catalytic activity. A series of diffraction lines for α-Co on X-ray diffraction patterns for Co-Mo-Zr deposits on steel substrates represent substitution solid solutions based on cobalt (Figure 5). No other phases including inter-metallic compounds were not found in the coatings' structure even after a 3-hour annealing the coated sample on the air at a temperature of 600 °C. Furthermore, one can find a wide halo (full width at half maximum is about 5°) at angles 2θ~59 °, which indicates an amorphous structure of above mentioned materials.
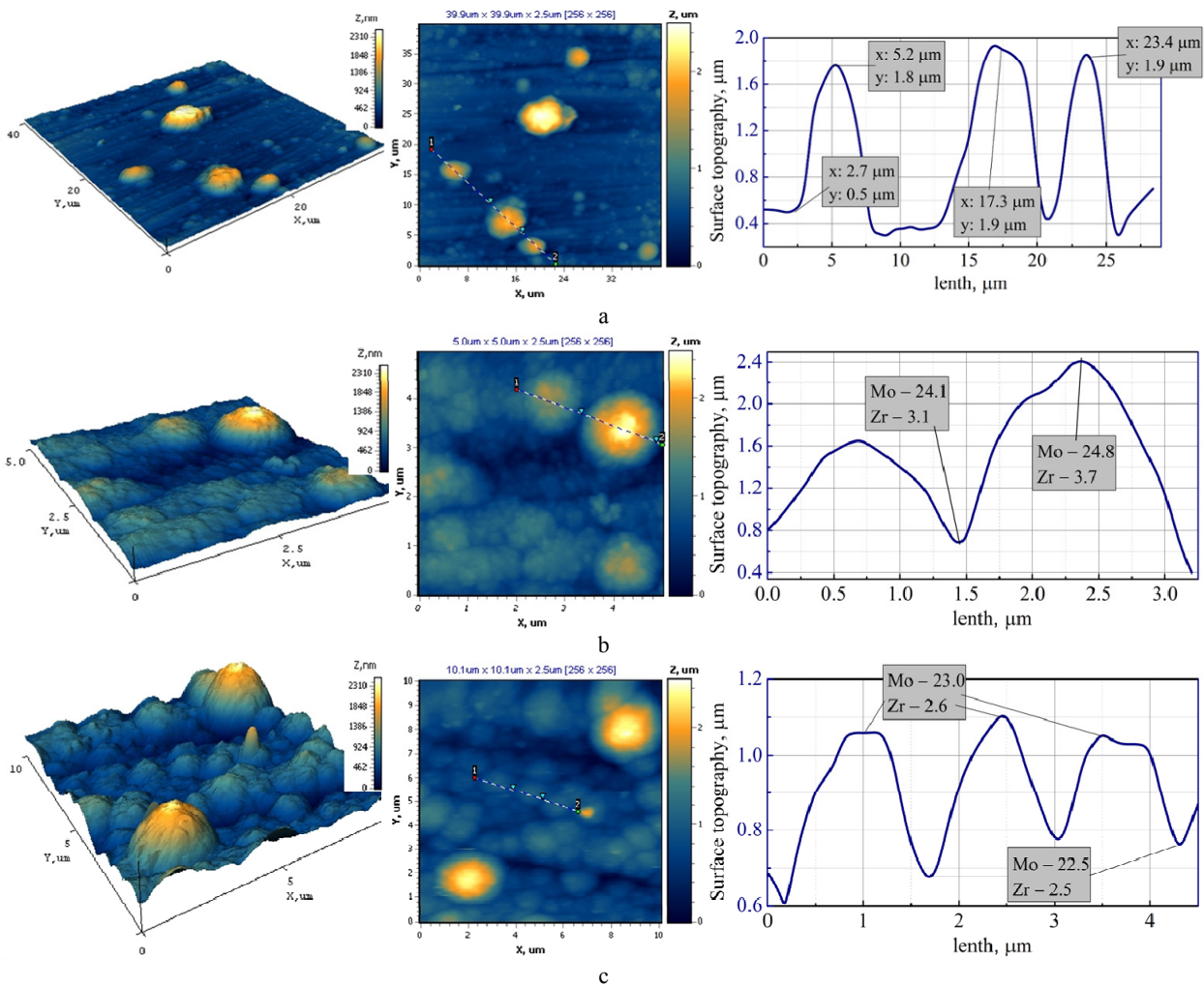
Figure 4 – 3D-. 2D-map and cross section of the surface Co-Mo-Zr between markers 1–2 deposited in pulse mode at current density 4 A·dm⁻² (a. b) and 6 A·dm⁻² (c); t_{on}/t_{off} = 2 / 10 ms; T = 25 °C; pH 8; plated time 30 min. Scan area AFM: a – 40x40 μm; b – 5.0x5.0 μm; c – 10x10 μm
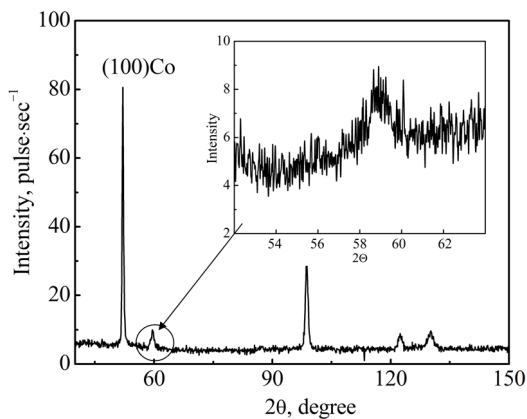
Figure 5 – X-ray diffraction patterns for deposit Co-Mo-Zr. the composition is similar to Figure 3 a (t_{on}/t_{off} = 2 / 10 ms)

Corrosion of cobalt based electrolytic coatings as it follows from the nature of alloying components proceeds predominantly with hydrogen depolarization in an acidic medium (Figure 6), and in neutral and alkaline under oxygen action. Corrosion potential of coatings alloyed with zirconium shifts in the negative direction in all environments (Figure 6, 7 Table 2) that agrees completely with the thermodynamic characteristics of zirconium. At the same time, the corrosion rate of a ternary alloy in the acidic and neutral chloride-containing environment declines by almost an order of magnitude compared with the binary system (Table 2). It can be explained by an increased tendency to passivity of zirconium-containing material as can be seen from the corrosion plots (Figure 6) and the geometry of the anodic

polarization dependences (Figure 7). Also ternary alloy increases resistance to pitting corrosion initiated with chloride ions. The difference in corrosion rate of Co-Mo and Co-Mo-Cr coatings in an alkaline environment is not as great due to the acidic nature of passive oxides of molybdenum and zirconium which reacting with hydroxide ions. According to the calculated depth corrosion index k_h synthesized binary alloys with a molybdenum content not less than 10 at% and ternary ones with a zirconium content of at least 2 at.% belong to the group 1 – "very proof".

Results of testing the catalytic activity of Mo-Co and Co-Mo-Zr alloy coatings in the model reaction of hydrogen evolution from different media (Table 3) indicate the synergistic nature of the electrolytic alloys. The exchange current density of hydrogen on the surface of binary and ternary alloys is higher than this parameter on alloying components which can be attributed obviously with the change in the mechanism of the process. From the literature [34-36] it is known that the hydrogen evolution on cobalt occurs by Volmer-Heyrovsky mechanism (b = −0.1 V) with the limiting discharge stage (Volmer), which is described for the acidic medium by reaction

$$H_3O^+ + e = H_{ad} + H_2O,$$
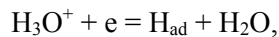
and for neutral and alkaline

$$H_2O + e = H_{ad} + OH^-.$$
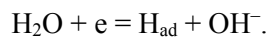
Reducing of hydrogen on the metals subgroups of molybdenum and titanium is described by the same sequence of steps. However, the limiting stage is electrochemical desorption (Heyrovsky step) occurring in an acid medium by reaction

$$H_3O^+ + H_{ad} + e = H_2 + H_2O,$$

and in neutral and alkaline

$$H_2O + H_{ad} + e = H_2 + OH^-.$$
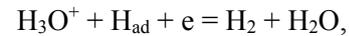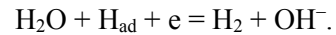
As seen from the coefficient b = 0.03 (Table 3) hydrogen evolution both on the electrolytic Co-Mo alloy in an acidic medium and on Co-Mo-Zr coating in an alkali medium are limited by recombination stage

$$H_{ad} + H_{ad} = H_2,$$

i.e. flows through the Tafel mechanism. The same mechanism is typical for platinum, this is evidence of the high catalytic activity of the materials studied.

Thus, the combination of metals with different limiting stage of hydrogen evolution in the active layer allows obtaining a material with catalytic activity close to platinum metals.

Testing of the catalytic activity of the synthesized Co-Mo-Zr coatings was also performed in the model reaction of carbon (II) oxide conversion to carbon (IV) oxide. Quantitative characteristics of the oxidation are the carbon (II) oxide conversion degree X(CO) and ignition temperature T_i. The catalytic properties of galvanic alloys were compared to platinum which is the most effective catalyst. As one can see from the temperature dependencies (Figure 7, 1) at the platinum plate catalyst with ω(Pt)=100 at.% the oxidation of CO begins at 190 °C, while 100 % conversion degree is achieved at 250 °C.
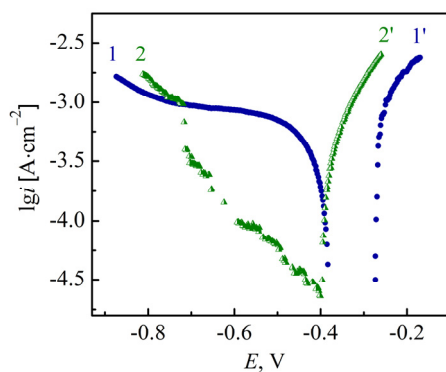
Figure 6 – Corrosion diagrams for coatings Co-Mo (1) and Co-Mo-Zr (2) in 1 M Na₂SO₄ (pH 3): cathodic plots (1. 2); anodic plots (1'. 2')
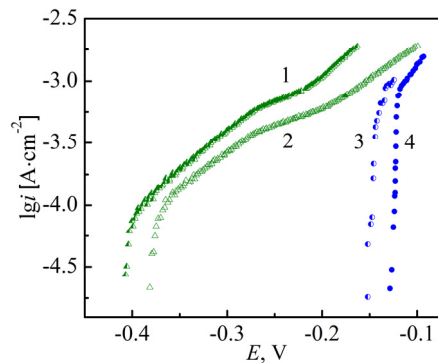
Figure 7 – Anodic polarization plots for coatings Co-Mo-Zr (1. 2) and Co-Mo (3. 4) in media: 1 M Na₂SO₄ pH 11 (1. 3); 3 % NaCl pH 7 (2. 4)
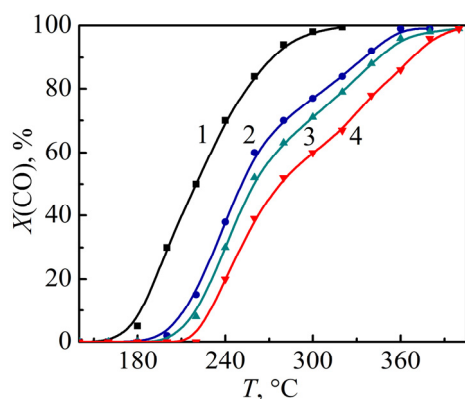
Figure 8 – Thermograms of CO conversion degree on Pt (1) and galvanic alloys Co-Mo-Zr of composition. wt .%: Co − 82.1. Mo – 17.1. Zr – 1.9 (2); Co − 83.0. Mo – 15.6. Zr – 1.4 (3); Co – 83.3. Mo – 15.8. Zr − 0.9 (4)

As can be seen from Figure 7, the thermograms of carbon (II) oxide conversion at the surface of catalyst coated with ternary alloys with various content of zirconium (dependences 2–4) have two sections with different slopes. In the first plot within the temperature interval 200–270 ℃ the kinetics of CO oxidation is not differ from the platinum plate catalyst with $\omega(Pt)$ =100 at.% although both the reaction initiation temperature T_{in} as well as temperature of 50 % conversion are higher than on platinum by 40–50 ℃ (Table 4). In the second plot at a temperature above 270 ℃ oxidation rate declines probably due to the formation of alloying metals oxides on the surface. The conversion degree rises by an average of 7–10% with increase the zirconium content in the coating by 1 at.% but the influence of zirconium weakens at the temperatures higher 350 °C. Evidence of high catalytic activity of materials is the fact that 99% conversion is achieved at temperatures of 375–380 °C. Catalytic properties of the synthesized systems are caused by cobalt ability to form nonstoichiometry oxides with different thermal resistance as well as by high affinity for oxygen of molybdenum and especially zirconium.

The above results are conclusive evidence not only of Co-Mo-Zr high catalytic activity but gives every reason to replace platinum catalysts at a cheaper galvanic alloys cobalt-molybdenum-zirconium an added benefit of which is a metallic substrate.

1. Binary and ternary alloys of cobalt with molybdenum (zirconium) of different composition and morphology are obtained from polyligand citrate-pyrophosphate electrolyte in a pulsed mode by varying the current density and temperature. It is shown that at a current density of not more than 3 A·dm^{-2} coatings with micro-globular topography without stress and cracks are formed. Electrolytic alloys are solid solutions of zirconium and tungsten in cobalt in the wide range of alloying metals concentrations.

2. Chemical resistance of binary and ternary coatings based on cobalt is caused by the increased tendency to passivity and high resistance to pitting corrosion in the presence of molybdenum and zirconium, as well as the acid nature of their oxides. Binary coating with molybdenum content not less than 10 at % and ternary ones with zirconium content in terms of corrosion deep index are in a group "very proof" and can be recommended as protective for corrosive environments.

3. Electrolytic Co-Mo and Co-Mo-Zr alloys demonstrated synergism of catalytic activity for the hydrogen reduction from various media. It is shown that the combination of metals with different limiting stage of hydrogen evolution allows obtaining a material with catalytic activity close to platinum metals.

4. Electrolytic alloy Co-Mo-Zr with a Zr content of not less than 1.5 at% exhibits catalytic activity in the oxidation of carbon (II) oxide. This allows you to recommend the synthesized materials to replace platinum catalysts for improving the efficiency of the combustion of hydrocarbons and purification of gas emissions from toxic substances.

Conclusions

(i) Uniform ternary coatings Co-Mo-Zr of different composition can be produced in a pulsed mode from the polyligand citrate-pyrophosphate bath by varying the energetic and time electrolysis parameters.

(ii) The electro-catalytic activity of the Co-Mo-Zr alloys comparing with individual metals exhibits their synergetic nature. The greatest level of catalytic properties was obtained on synthesized alloys in acidic media for which the hydrogen exchange current density do not differ from the parameter for a platinum electrode.

(iii) The galvanic alloys Co-Mo-Zr with zirconium content 1.5–2.0 at.% exhibit high catalytic properties in the carbon oxide (II) oxidation. This confirms the efficiency of materials as catalysts for the gaseous wastes purification and

gives the reason to recommend them as catalysts for hydrocarbon combustion.

References

1. J. Larminie, A. Dicks. Fuel cell systems explained // 2nd ed. John Wiley & Sons Ltd. – Chichester. – 2003. – P. 121–137.

2. K. Tomantschger, K. V. Kordesch. Structural analysis of alkaline fuel cell electrodes and electrode materials // J. Power Sources. – 1989. – Vol. 25. – P. 195–214

3. M. Skyllas-Kazakos, M. H. Chakrabarti, S.Hajimolana et al. Progress in flow battery research and development // J. Electrochem. Soc. – 2011. – Vol. 158. – P. R. 55–R79.

4. S.M. Haile. Fuel cell materials and components // Acta Materialia. – 2003. – Vol. 51. – P. 5981–6000

5. Mustakeem. Electrode materials for microbial fuel cells: nanomaterial approach // Mater Renew Sustain Energy. – 2015. – P. 22.

6. S. Litster1, G. McLean. PEM fuel cell electrodes // Journal of Power Sources. – 2004. – Vol. 130. – P. 61-76.

7. S. Chen, H.A. Gasteiger, K. Hayakawa, T. Tada, Y. Shao-Horn. Platinum-Alloy Cathode Catalyst Degradation in Proton Exchange Membrane Fuel Cells: Nanometer-Scale Compositional and Morphological Changes // J. Electrochem. Soc. – 2010. – Vol. 157. – P. A82-A97

8. C. Ponce de Leon, A. Frias-Ferrer, A. Gonsales-Garcia et al. Redox flow cells for energy conversion // Review. J. Power Sources. – 2006. – Vol. 160. – P. 716–732.

9. A.Z. Weber, M.M. Mench, J.P. Mejers et al. Redox flow batteries // J. Appl. Electrochem. – 2011. – Vol. 41. – P. 1137–1164.

10. H.M. Tsai, S.Y. Yang, C.M. Ma, X. Xie. Preparation and electrochemical properties of graphene-modified electrodes for all-vanadium redox flow batteries // Electroctrocatalysis. – 2011. – Vol. 23. – P. 2139–2143.

11. T.D. Hatchard, J.E. Harlow, K.M. Cullen, R.A. Dunlap, J.R. Dahn. Non–Noble Metal Catalysts Prepared from Fe in Acid Solution // J. Electrochem. Soc. – 2012. – Vol. 159. – P. B121-B125

12. Y. Chino, K. Kakinuma, D. A. Tryk, M. Watanabe, M. Uchida. Influence of Pt Loading and Cell Potential on the HF Ohmic Resistance of an Nb-Doped SnO_2-Supported Pt Cathode for PEFCs // J. Electrochem. Soc. – 2016. – Vol. 163. –P. F97-F105

13. E. Vernickaite, N. Tsyntsaru, H. Cesiulis. Electrodeposited Co-W alloys and their prospects as effective anode for methanol oxidation in acidic media // Surf. and Coat. Techn. In Press

14. G. Yar-Mukhamedova. Modified electrolytic Cr-based composite coatings // Materials Sciense. – 1999. – Vol. 35. – P. 601-608.

15. R. Ramanauskas, L. Gudavičiūtė, R. Juškėnas. Effect of pulse plating on the composition and corrosion properties of Zn–Co and Zn–Fe alloy coatings // Chemija. – 2008. – Vol. 19. – P. 7-13.

16. M.V. Ved', N.D. Sakhnenko, A.V. Karakurchi, S.I. Zyubanova. Electrodeposition of Iron–Molybdenum Coatings from Citrate Electrolyte // Russian Journal of Applied Chemistry. – 2014. – Vol. 87. – P. 276−282.

17. I. Shao, P.M. Vereecken, C.L. Chien, R.C. Cammarata, P.C. Searson. Electrochemical Deposition of FeCo and FeCoV Alloys // J. Electrochem. Soc. – 2003. – Vol. 150. – P. C184-C188.

18. N. Tsyntsaru, H. Cesiulis, A. Budreika. The effect of electrodeposition conditions and post-annealing on nanostructure of Co–W coatings. Surf. Coat. Technol. – 2012. – Vol. 206. – P. 4262-4269.

19. D.Z. Grabco, I.A. Dikusar, V.I. Petrenko, E.E. Harea. Micromechanical Properties of Co–W Alloys Electrodeposited under Pulse Conditions // Surf. Eng. and Applied Electrochemistry. – 2007. – Vol. 43. – P. 11–17.

20. G. Yar-Mukhamedova, M. Ved', N. Sakhnenko. A. Karakurkchi, I. Yermolenko. Iron binary and ternary coatings with molybdenum and tungsten // Appl. Surf. Sci. – 2016. – Vol. 383. – P. 346-352

21. M. Ved', M. Glushkova, N. Sakhnenko. Catalitic properties of binary and ternary alloys based on silver // Functional Materials. – 2013. – Vol. 20. – P. 87–91.

22. O.A. Petrii. Electrosynthesis of nanostructures and nanomaterials // Russian Chemical Reviews. – 2015. – Vol. 84. – P. 159–193.

23. T. Nenastina, T. Bairachnaya, M.Ved' et al. Electrochemical synthesis of catalytic active alloys // Functional Materials. – 2007. – Vol. 14. – P. 395-400.

24. V.S. Kublanovsky, Yu.S. Yapontseva. Electrocatalytic Properties of Co-Mo Alloys Electrodeposited from a Citrate-Pyrophosphate Electrolyte // Electrocatalysis. – 2014. – Vol. 5. – P. 372-378.

25. M.A. Glushkova, T.N. Bairachna, M.V. Ved, N.D. Sakhnenko. Electrodeposited cobalt alloys as materials for energy technology // Mater. Res. Soc. Symp. Proc. USA. – Boston. – 2013. – Vol. 1491.

26. G.S. Yar-Mukhamedova. Influence of thermal treatment on corrosion resistance of chromium and nickel composite coatings. Materials Science. – 2000. – Vol. 36. – P. 922-929.

27. Komarov F, Ismailova G, Yar-Mukhamedova G. Effect of thermal processing on the structure and optical properties of crystalline silicon with GaSb nanocrystals formed with the aid of high-doze ion implantation // Technical Physics. – 2015. – Vol. 60. – P. 1348-1352.

28. G.S. Yar-Mukhamedova. Investigation of the Texture of Composite Electrodeposited Chromium–Carbon Coatings // Materials Sciense. – 2000. – Vol. 36. – P. 752-759.

29. M. Ved', N. Sakhnenko. M. Glushkova. T. Bairachna. Electrodeposition of functional cobalt-silver and cobalt-tungsten alloys // Chemistry & Chemical Technology. – 2014. – Vol. 8. – P. 275-281.

30. M.O. Glushkova, M.V. Ved, M.D. Sakhnenko. Corrosion Properties of Cobalt–Silver Alloy Electroplates // Mater. Sci. – 2013. – Vol. 49. – P. 292–297.

31. G. Yar-Mukhamedova. Internal adsorption of admixtures in precipitates of metals // Materials Sciense. – 1999. – Vol. 35. – P. 598-610.

32. E.J. Podlaha. Induced codeposition: III. Molybdenum alloys with nickel. cobalt and iron // J. of the Electrochemical Society. – 1997. – Vol. 144. – P. 1672–1680.

33. G.S. Yar-Mukhamedova. Investigation of corrosion resistance of metallic composite thin-film systems before and after thermal treatment by the "Corrodkote" method // Materials Science. – 2000. – Vol. 37. – P. 140-149.

34. J. Li, S. Meng, J. Han, X. Zhang. Valence electron structure and properties of the ZrO_2. Sci // China Ser. E-Technol. Sci. – 2008. – Vol. 51. – P. 1858-1866.

35. M.R. Gennero, A.C. Chialvo. Kinetics of hydrogen evolution reaction with Frumkin adsorption: Re-examination of the Volmer-Heyrovsky and Volmer-Tafel routes // Electrochimica. – 1998. – Vol. 44. – P. 841–851.

36. A.V. Karakurkchi, M.V. Ved', N.D. Sakhnenko et.al. Functional properties of multicomponent galvanic alloys of iron with molybdenum and tungsten // Functional Materials. – 2015. – Vol. 22. – P. 181–187.